The Plant Journal (2007) **50**, 637–648 doi: 10.1111/j.1365-313X.2007.03074.x

Transcriptome profiling of maize anthers using genetic ablation to analyze pre-meiotic and tapetal cell types

Jiong Ma, David Duncan[†], Darren J. Morrow, John Fernandes and Virginia Walbot[*]
Department of Biological Sciences, Stanford University, Stanford, CA 94305-5020, USA

Received 9 November 2006, revised 10 January 2007, accepted 18 January 2007
[*]For correspondence (fax: +1 650 725 8221; e-mail: walbot@stanford.edu).
[†]Present address: 353 Aldean Ave, Mountain View, CA 94043, USA.

Summary

Oligonucleotide arrays were used to profile gene expression in dissected maize anthers at four stages: after-anther initiation, at the rapid mitotic proliferation stage, pre-meiosis, and meiotic prophase I. Nearly 9200 sense and antisense transcripts were detected, with the most diverse transcriptome present at the pre-meiotic stage. Three male-sterile mutants lacking a range of normal cell types resulting from a temporal progression of anther failure were compared with fertile siblings at equivalent stages by transcription profiles. The *msca1* mutant has the earliest visible phenotype, develops none of the normal anther cell types and exhibits the largest deviation from fertile siblings. The *mac1* mutant has an excess of archesporial derivative cells and lacks a tapetum and middle layer, resulting in moderate transcriptional deviations. The *ms23* mutant lacks a differentiated tapetum and shows the fewest differences from fertile anthers. By combining the data sets from the comparisons between individual sterile and fertile anthers, candidate genes predicted to play important roles during maize anther development were assigned to stages and to likely cell types. Comparative analyses with a data set of anther-specific genes from rice highlight remarkable quantitative similarities in gene expression between these two grasses.

Keywords: anther, development, transcriptome, male-sterile, flower.

Introduction

All plants lack a germ line of cells dedicated to reproduction, and in angiosperms only late in floral development do cells within the developing anther differentiate as microsporocytes, and subsequently undergo meiosis (Ma, 2005). The ABC model for floral organ identity, mostly based on studies of the homeotic MADS-box genes from Arabidopsis and Antirrhinum, provides the framework for understanding early steps in floral ontogeny (Jack, 2004). Considerable progress has also been made in understanding the late processes in anther development, including meiosis, microsporogenesis and pollen maturation (Ma, 2005). To date, however, little is known about either the mechanism of microsporocyte progenitor specification or the signaling events that induce the initiation of meiosis in these cells.

Anthers typically contain four somatic cell layers encircling the sporogenous cells within each anther locule (Goldberg *et al.*, 1993). In maize anther primordia, the outer (L1) layer produces the epidermis (Figure 1a). The inner (L2) hypodermal cells divide periclinally to produce archesporial cells internally and primary parietal cells externally. The primary parietal cells again divide periclinally: the subepidermal layer differentiates into endothecium, and the inner secondary parietal layer divides to form the middle layer externally and the tapetum internally. Archesporial cells proliferate for several generations before committing to microsporocyte differentiation. This is a chronology of anther development, but its implication that lineage determines cell identity conflicts with the emerging consensus on the mechanisms of cell fate determination in plants. Evidence from mosaic and genetic analyses has suggested that interactions and signaling between cell populations determine cell fate during organogenesis, especially in the specification of cell-type identities (Irish and Jenik, 2001; Ma, 2005).

Here maize male-sterile (*ms*) mutants are used to study molecular events before meiosis. Although male sterility is common in flowering plants, the majority of mutants affect pollen maturation with defects after meiosis. By evaluating

the detailed cytological descriptions of ~40 maize *ms* mutants, several were identified in which stamen specification and filament differentiation occur normally, but either one or more anther cell types fails to differentiate appropriately before the onset of meiosis. Advantageous for anther dissection, the maize tassel contains only male flowers, thousands of anthers are at the same developmental stage and nearly all *ms* mutants are female-fertile. Comparing the transcriptomes of such mutants with their fertile siblings at stages before, during and after the time when cytological differences were apparent, should begin to define the hierarchy of gene expression required for normal anther development.

Three *ms* mutants with distinct temporal and tissue defects were selected (Figure 1a,b). The most severe is *male sterile converted anther1* (*msca1*, originally *ms22*; Chaubal *et al.*, 2003). Although stamen primordia initiate properly and a normal filament is produced, *msca1* anthers ultimately lack all expected cell types. Instead, the anther becomes a stem-leaf-like organ in which the epidermis contains stomata; parenchyma and non-functional vascular strands are formed in the interior (Chaubal *et al.*, 2003). In the *multiple archesporial cells1* (*mac1*) mutant, primary parietal cells fail to complete either one or more periclinal divisions; as a consequence, the middle and tapetal layers are either missing or perhaps differentiate as archesporial cells. At the initiation of meiosis, archesporial cells of varying sizes and shapes fill the locule; meiosis aborts in prophase I (Sheridan *et al.*, 1999). Finally, the *ms23* mutant forms all cell layers normally, but the tapetum precursor cells undergo an additional periclinal division and tapetal differentiation fails. The sporogenous cells enter meiosis but degenerate before completing meiosis I (Chaubal *et al.*, 2000). These *ms* mutants should prove informative for the crucial cell-fate decisions that result in meiotically competent cells and somatic cell types, especially the tapetum.

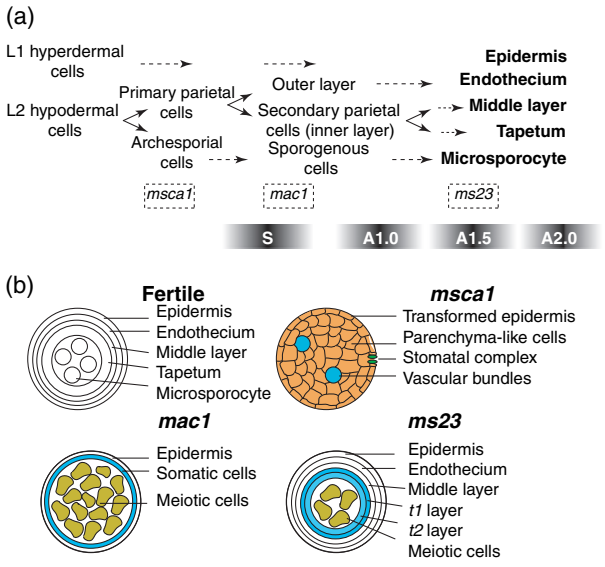

Figure 1. Anther cell type differentiation.
(a) Lineages in maize with differentiated cell types in bold. The boxed mutant names indicate the onset of visible defects for each *ms* mutant. The stages of tissue dissected are displayed with shaded boxes: S, spikelets (including young anthers < 0.5 mm in length); A1.0, 1.0-mm anther; A1.5, 1.5-mm anther; A2.0, 2.0-mm anther.
(b) Diagrams of transverse sections of fertile and *ms* anther locules, idealized as circles. The fertile anther is shown at meiosis, whereas the mutants are shown at their terminal phenotype. Meiosis aborts during prophase I in *mac1* and before the completion of meiosis I in *ms23*.

Results

Biological materials, microarray design and data validation

Using Version 1 Agilent 22 K maize arrays, the transcriptomes of fertile anthers at mitotic and just pre-meiotic stages were found to be highly conserved in three backgrounds: W23, an A619 derivative and the W23/ND101 hybrid (Ma *et al.*, 2006). This fact simplifies comparisons among mutants in these backgrounds. The *ms23* and *msca1* lines used here were self-pollinated progeny of *ms*//+ in W23/ND101-segregating one-quarter *ms*. The *mac1* plants came from families segregating either 1:1 (*mac1*//*mac1* × *mac1*//+) or 3:1 (*mac1*//+ × self) *ms* in the A619 derivative background. Anthers were dissected from upper florets from part of a developing tassel, and the remaining parts matured to permit later classification of fertility (see Experimental procedures). Based on cytological staining to classify development (data not shown), three lengths were selected: the mitotic proliferation stage at 1.0 mm (A1.0 stage); at 1.5 mm (A1.5) most sporogenous cells are about to enter meiosis; at 2.0 mm (A2.0) most microsporocytes are in prophase I (Figure 1a). Although there is a slight gradient of differentiation within an anther, each dissected stage is discrete. Immature spikelets (S), with anthers <0.5 mm were also dissected. *msca1* show morphological differences from normal as early as the 1.5-mm stage, whereas both *mac1* and *ms23* are slightly shriveled compared with fertile anthers at the 2.0 mm stage. Mutant anthers also senesce prematurely.

Version 2 Agilent 22 K arrays contain 20 963 gene features (~13 000 unique sense and ~5000 unique antisense transcripts) and share 17 026 probes with Version 1, thereby permitting validation of results for thousands of probes at the A1.0 and A1.5 stages. Of the shared probes, 11 455 were deemed 'non-hybridizing' on Version 1 and 10 153 were 'non-hybridizing' on Version 2 for these stages. Remarkably, 9919 probes were called present on both arrays, indicating great consistency between the two array experiments. We note that the thresholds for the Version 2 analysis were more relaxed, attributable to improved efficiencies in array handling and hybridization that reduced systematic variations. Of the 'hybridizing' probes, an extremely high correlation in the

normalized relative expression levels was found between the two array versions using a final subset of 5175 hybridizing probes in both experiments (see Experimental procedures). As shown in Figure 2(a,b), the comparisons between the *ms23* fertile tissues and the ND101/W23 hybrid tissues achieved correlation coefficients of 0.93 and 0.92, for the A1.0 and A1.5 stages, respectively. Other tissue comparisons also showed comparably high correlations (all >0.85; data not shown). Previously, a relatively large set of quantitative real-time PCR (qRT-PCR) validation experiments (Ma *et al.*, 2006) also confirmed a subset of the results.

To identify internal standards for microarray and qRT-PCR analyses in maize anthers, four candidates were selected by the method of Czechowski *et al.* (2005): a histone acetyltransferase (*GCN5*; TIGR: TC326475), a helicase-domain-containing gene (GenBank: BG833488), a cyanate hydratase (TIGR: TC330555) and a ubiquitin-conjugating enzyme gene (*UBC*; GenBank: BG836869). Of these, the helicase-domain and *UBC* genes have Arabidopsis homologs that were identified as good universal controls (Czechowski *et al.*, 2005). qRT-PCR was performed in triplicate on either two or three biological replicates of both the fertile and male-sterile samples for *ms23* and *msca1*. Cyanase displayed the most consistent array hybridization signals across all stages inspected, and was used as an internal standard for the other three genes to calculate $\Delta C_t = C_t(\text{sample}) - C_t(\text{standard})$ (C_t, cycle threshold). The ΔC_t value is a normalized relative expression value, parallel to a log-2 ratio because of the doublings in PCR reactions. A polynomial regression analysis found a significant positive correlation between the qRT-PCR and array results ($r^2 = 0.82$; Figure 2c). This validates both the array results and use of these genes as internal standards for future experiments with maize anthers.

The third validation used three of the 24 sample types (S stage *msca1* plus fertile siblings at stages A1.0 and A1.5) with four biological replicates each hybridized to Affymetrix GeneChip® Maize Genome Arrays. In total 2636 Affymetrix probe sets overlapped in the same orientation with positively hybridizing probes on the Agilent platform. The Pearson correlation coefficients between the two sets of expression values ranged from 0.47 to 0.49 (Data S1). This correlation is lower than previous comparisons between Agilent platforms and between Agilent Version 1 and spotted 70-mer arrays (Ma *et al.*, 2006). There are fundamental differences between a single 60-mer probe (the Agilent platform) and fifteen 25-mer probes (the Affymetrix platform) and the algorithms to normalize hybridization signals. The most variations occur with low expression transcript types identified by the Agilent arrays, which displayed a wide range of expression values on the Affymetrix platform (Data S1). On the other hand, the Agilent array results agreed well with the low expression class identified

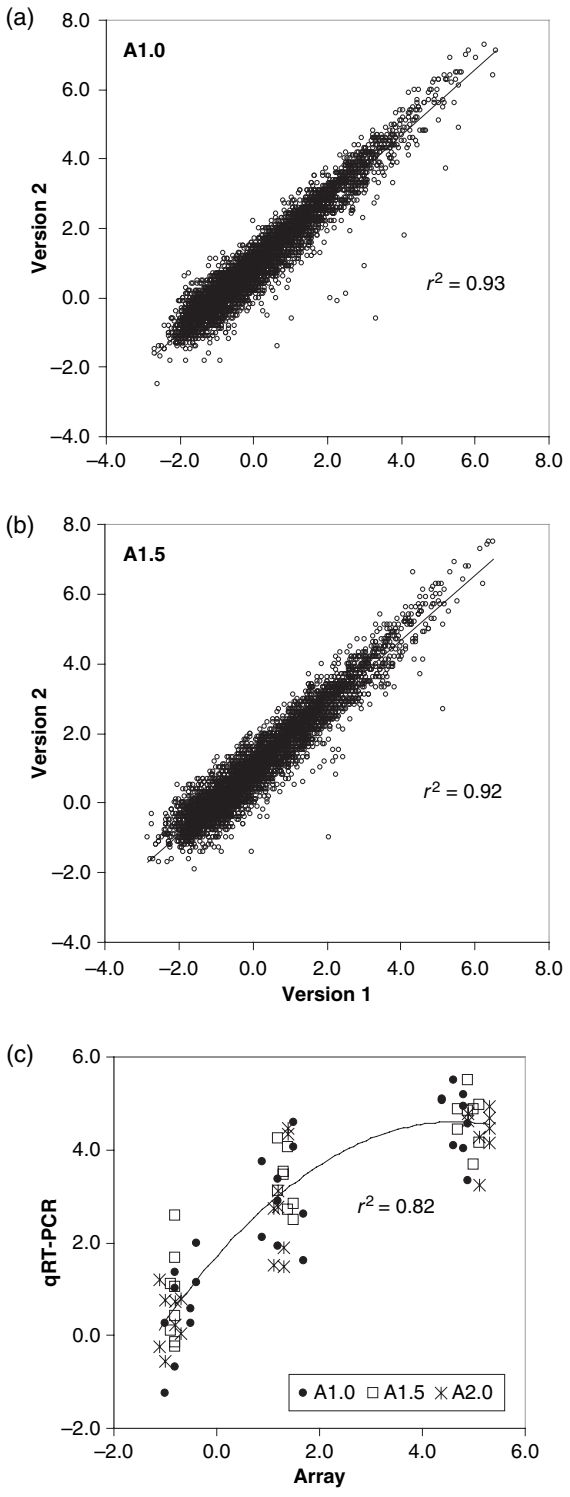

Figure 2. Validation of array results. Correlations between array results from Version 1 and Version 2 Agilent arrays are shown for (a) A1.0 (1.0-mm anther) and (b) A1.5 (1.5-mm anther) stages for the fertile siblings of *ms23*.
(c) Correlation between array results and quantitative real-time PCR (qRT-PCR) ΔC_t (C_t, cycle threshold) values for proposed internal control transcripts across the three anther stages. The three transcripts are (from left to right): the helicase-domain gene, *GCN5* and *UBC*.

on Affymetrix chips (Data S1). Even though multiple probes could minimize sequence-dependent false negatives, the low expression class has been shown to be problematical for gene-chip analysis (Barnes *et al.*, 2005); as shown in Figure 2(a–c), the 60-mer oligo arrays are very consistent across multiple tissue types and biological samples, and also have been validated repeatedly by qRT-PCR. Therefore, longer probes are a superior solution for transcriptome profiling of multiple lines from a species like maize with duplicated and highly polymorphic alleles (Walbot and Petrov, 2001).

Most transcripts are shared among the anther stages

Absolute gene expression levels in the four fertile stages were compared. To reduce systematic errors inevitably associated with array experiments, probes were considered that showed significant hybridization signals in at least two out of the three backgrounds at each stage. Altogether, about 9200 sense (93%) and antisense (7%, within sense transcription units) transcripts represented by 10 693 probes were detected in these stages. About 6800 (74%) transcripts were found at all four stages, including 'housekeeping' genes, such as those shared with the leaf (Ma *et al.*, 2006) and floral-specific transcripts. Temporal patterns of gene expression involve ~2400 transcriptome changes with the most diverse transcriptome present at A1.5 (Figure 3a). Each stage was evaluated relative to the preceding stage to define transcripts that persist, that are induced or that disappear as development progresses. There are ~200 stage-specific (called 'present' only in a given stage) transcripts in the A1.0 stage, ~300 for A1.5 and ~100 for A2.0. It is striking that the 1.0–1.5-mm transition, which spans only ~12 h, is accompanied by major transcriptome changes.

Previously 456 antisense transcripts were identified in A1.0 and A1.5 (Ma *et al.*, 2006). In the current study, their expression was corroborated, and with the addition of S and A2.0 additional antisense transcripts were detected on Version 2 arrays. Among the ~700 antisense transcripts found, 229 were detected in all four developmental stages. In parallel with sense transcripts, A1.0 and A1.5 express the greatest number of antisense transcripts (Figure 3b). Moreover, many antisense transcripts (244) disappeared between A1.5 and A2.0, resulting in a dramatic reduction in the number of antisense transcripts during meiosis (Figure 3b). The significance of this change is unclear, as the functions of these antisense transcripts are presently unknown. Furthermore, few antisense transcripts are co-expressed with the counterpart sense RNA, as described in detail in Ma *et al.* (2006).

Transcriptome deviations from wild type in ms mutants correlate well with the onset of visible phenotypes

Figure 4(a) displays the number and dynamics of differentially expressed genes in each mutant. All of the differentially expressed genes are listed in Data S2. In all three mutants, the largest number of differentially expressed sense transcripts was found at stage A1.5 (Figure 4a), when fertile anthers have the most complex transcriptome.

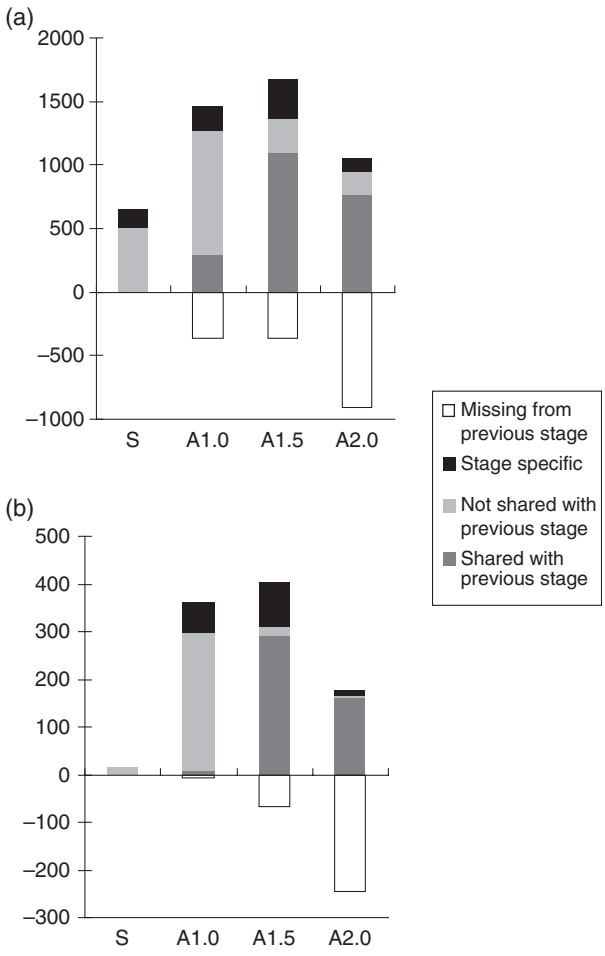

Figure 3. Transcriptome components of fertile siblings for (a) total transcripts and (b) antisense transcripts. The ~6800 transcripts shared by all four stages are not shown in (a). S, spikelets (including young anthers < 0.5 mm in length); A1.0, 1.0-mm anther; A1.5, 1.5-mm anther; A2.0, 2.0-mm anther.

Relative to fertile tissues, at stage A1.0 *msca1* anthers differentially express 247 genes, many of which remain abnormally expressed at later stages, with progressively more differences accumulating at later stages (Figure 4a). *mac1* anthers display dynamics similar to *msca1*, although with fewer changes (Figure 4a). Interestingly, differential gene regulation shows greater stage specificity in *mac1* than in *msca1*: 119 (67% of differentially expressed genes at A1.0) differed from fertile sibling expression levels only in A1.0, 279 (80%) in A1.5 and 76 (54%) in A2.0, compared with 71 (29%), 192 (45%) and 126 (37%) in *msca1*, at the same stages. Consistent with observations of normal and *msca1* anthers, the A1.5 stage of *mac1* had the most

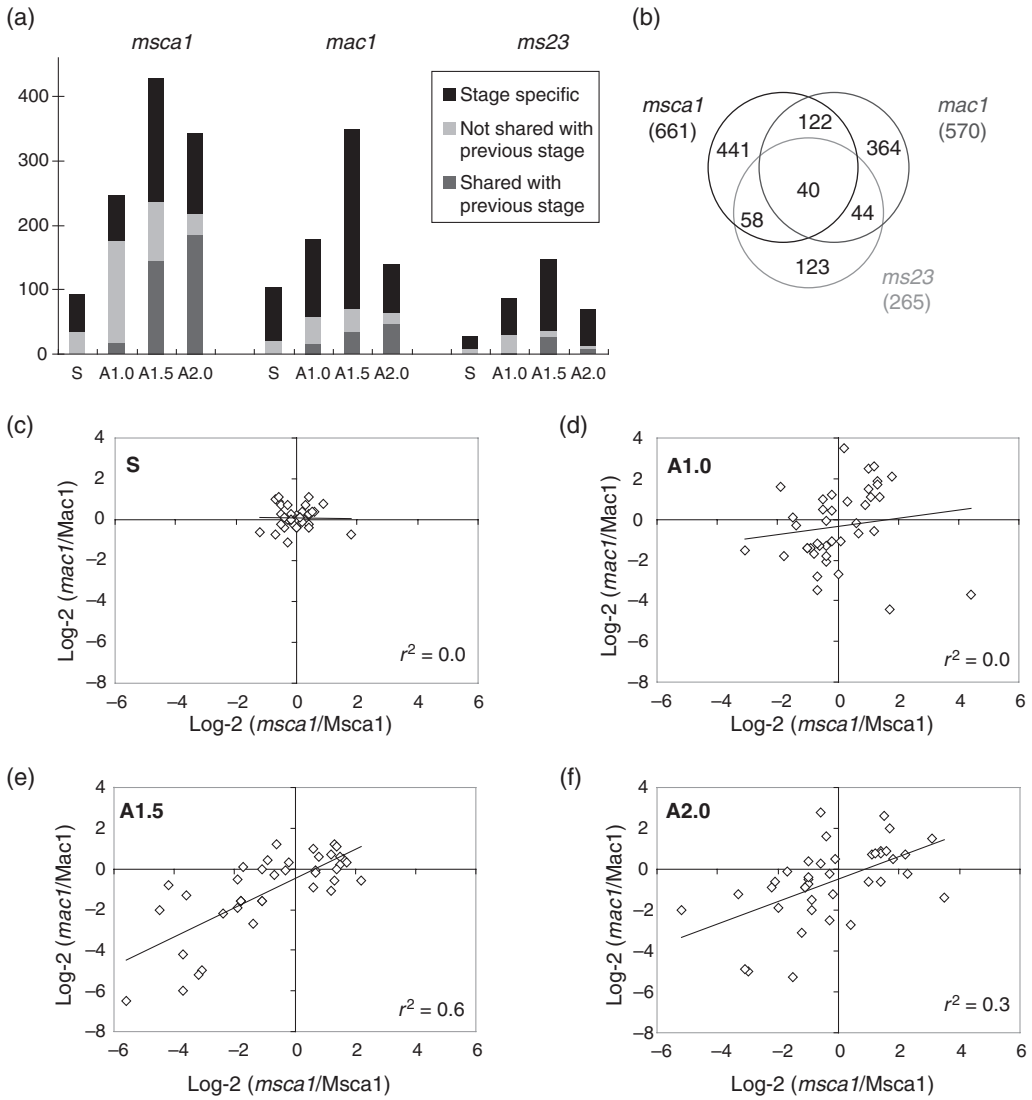

Figure 4. Distribution of differentially expressed genes in the three *ms* mutants. (a) The number of differentially expressed (either significantly up- or downregulated) sense transcripts in the three *ms* mutants compared with their fertile siblings. Very few (three on average) antisense transcripts were differentially expressed (not shown). (b) Overlap between the mutants in their differentially expressed genes for A1.0 (1.0-mm anther), A1.5 (1.5-mm anther) and A2.0 (2.0-mm anther) stages combined. (c–f) Correlations of log-2 ratios of mutant over fertile siblings between *mac1* and *msca1* anthers at the four stages within the 40 transcripts differentially expressed in all three *ms* mutants, as shown in (b). r^2 is the correlation coefficient.

significant changes, followed by a drop in differentially regulated genes at A2.0 (Figure 4a), reinforcing that stage A1.5 may serve as a decision point for certain developmental processes. The trend is identical in *ms23*, which acts later in development, except that *ms23* displayed about half as many differentially regulated genes as either *mac1* or *msca1* (Figure 4a).

Distinctive and shared features of transcriptomes of the male-sterile mutants

A Venn diagram highlights these genes differentially regulated by each mutant in at least one of the anther stages (Figure 4b). In both *msca1* and *mac1*, ~65% of differentially expressed transcripts were mutant-specific (441 and 364, respectively); in *ms23* there are 46% (Figure 4b). Forty transcripts were differentially expressed by all three mutants, and pairs of mutants shared from 122 (*msca1* and *mac1*) to 44 (*mac1* and *ms23*) differentially expressed genes (Figure 4b). As both mutants in this latter pair lack a tapetal layer, the shared differentially regulated transcripts should include genes required for late pre-meiotic steps in tapetal differentiation and responses in other cell types contingent on tapetal cells.

The relationship between the *ms* and fertile tissues was further explored by a hierarchical clustering of 3616 probes with above-median (after normalization) hybridization signals. In the resulting tree, 18 of 22 clusters were statistically

significant (≥ 95%) indicating a robust topology (Data S3). All S stages cluster together; also each mutant was more similar to its corresponding fertile siblings at the S stage than at any subsequent stage, indicating minimal changes at the S stage. The three anther stages of *msca1* form a separate cluster, indicating a relatively large deviation from normal. The anther stages of *mac1* and *ms23* also form discrete clusters, but are significantly more similar to fertile anthers than *msca1* (Data S3). This clustering tree strengthens the hypothesis that mutant anthers are still developmentally very close to normal. Even *msca1* expresses most of the common anther transcriptome across all three stages examined: *msca1* is not a complete homeotic conversion to stem-leaf organs but represents an anther with some leaf-like characteristics.

To further test for 'vegetative organ' identity in *msca1* a comparison was made with the juvenile leaf transcriptome (Ma *et al.*, 2006). Subgroups of differentially regulated genes were selected to minimize background noise (see Data S4 for details). For *msca1*, about 30% of the upregulated subgroups at all three anther stages are either moderately or highly expressed in juvenile leaf (Data S4a). *msca1* anthers express photosynthesis-related transcripts, including the Photosystem I P700 chlorophyll, an apoprotein A2 gene (*PsaB*), the NADH dehydrogenase 27-kDa subunit gene and the NADP-dependent malate dehydrogenase required for photosynthesis. Additionally, *msca1* anthers expressed a number of genes associated with senescence (Data S5). Such a high match was not found for the *mac1* anther data (Data S4b). *ms23* displayed upregulation of some senescence genes, but at a later stage and to a lesser extent (Data S4c). This may correlate with the later onset of the mutant deficiency and anther senescence.

A pairwise correlation analysis on the log-2 ratios (*ms* over fertile siblings) was also conducted within the transcript subsets defined in Figure 4(b). A high correlation coefficient would indicate similar regulation patterns between the *ms* mutants. Figure 4(c–f) display results for *msca1* and *mac1* anthers on the 40 transcripts shared among all three mutants (Figure 4b). It is immediately apparent that at the S stage, very few of the transcripts are differentially regulated in either mutant (Figure 4c). By the A1.0 stage more transcripts show significantly altered expression (Figure 4d), however, the regulation patterns are not correlated between the two mutants. At the A1.5 stage, a positive correlation in gene regulation is found between *msca1* and *mac1*, indicated by a linear regression line (r^2 = 0.6; Figure 4e). This correlation diminishes at the A2.0 stage (r^2 = 0.3; Figure 4f). Subsequently the same analysis was performed between other pairs of *ms* mutants and for other subsets of transcripts. The results are summarized in Table 1. Interestingly, there is a consistently high correlation in regulation patterns for the A1.5 stage, implying the existence of a suite of genes, many belonging to the 40 shared transcripts, which are regulated similarly in all three *ms* mutants at the switch-point A1.5 stage. It is likely that some of these genes are involved in tapetal differentiation, which is defective in all three mutants.

Expression of MADS-box genes important in stamen development

MIKC-type MADS-box genes with a role in stamen initiation and organ identity determination were expressed similarly in fertile and mutant anthers. Three of the four predicted maize B class genes were examined: S*ilky1* (*Si1*) and *ZMM16*, maize orthologs to the Arabidopsis B class genes *APETALA3 (AP3)* and *PISTILLATA (PI)* respectively (Ambrose *et al.*, 2000; Munster *et al.*, 2001; Whipple *et al.*, 2004), and *ZMM18* (Munster *et al.*, 2001). *Si1* displayed the highest expression level throughout the four stages. It and the less abundant *ZMM16* continually increased during anther development; *ZMM18* had a very similar expression profile, except for a lower level at S (data not shown). The expression profiles of these genes are remarkably similar in all three mutants. *ZAG1*, known to be expressed early in stamen and carpel primordia (Schmidt *et al.*, 1993), and *ZMM2* perform C/D function in maize, and were stably expressed at a low level in all fertile, *ms23* and *mac1* anthers, but were upregulated in *msca1* anthers. These are the only MADS-box genes of 20 on the array (out of a total of 34 in maize) to be significantly different in any mutant. The expression levels of the maize MADS-box genes were also evaluated in juvenile leaf using published data (Ma *et al.*, 2006). There are 10 transcripts

Table 1. Quantitative analysis of similarities in differential regulation between *ms* mutants.

Transcripts set	Correlation between	S	A1.0	A1.5	A2.0
Shared among all three mutants (40)	*msca1* : *mac1*	0	0	0.6	0.3
	ms23 : *mac1*	0	0.4	0.3	0.1
	msca1 : *ms23*	0	0.1	0.4	0.1
Shared between *msca1* and *mac1* only (122)	*msca1* : *mac1*	0	0.1	0.2	0.3
Shared between *mac1* and *ms23* only (44)	*ms23* : *mac1*	0	0.4	0.4	0
Shared between *msca1* and *ms23* only (58)	*msca1* : *ms23*	0.1	0.5	0.4	0.1

Using the sets of shared differentially regulated transcripts from Figure 4(b), the Pearson correlation coefficients (r^2) were determined between each *ms* pair on the log-2 ratios of *ms*:fertile for each anther stage.

(*ZMM3*, *ZMM27*, *ZAG3*, *ZMM28*, *ZmMADS3*, *ZAP1*, *ZAG1*, *Si1*, *ZMM16,* and *ZMM18*) shared between the two array platforms, and they showed very good correlation in expression values for the A1.0 and A1.5 stages (data not shown). In contrast, these MADS-box genes were undetected in either mature pollen or juvenile leaf, except for *Si1*, which had minimal pollen expression, in agreement with published data on spatial expression patterns for these genes.

Maize homologs of genes regulating B and C class genes – a *WUSCHEL* (*WUS*) homolog (TIGR:TC294225), a *HUA1* homolog (TIGR:TC306397), a *HUA enhancer2* (*HEN2*)-like gene (TIGR:TC298405) and a *HEN1* homolog (TIGR:TC289846) – were all expressed at low levels in both mutant and fertile anthers (data not shown). These genes are positive regulators of *AGAMOUS (AG)* (Ma, 2005) and presumably *ZMM2* in maize. *ZFL1* and TIGR:TC305378, maize homologs of two other positive regulators of *AG*, *LEAFY* (*LFY*) and *HEN4*, respectively, did not show detectable expression (data not shown). Transcripts of four maize *SEUSS* (*SEU*) homologs, negative regulators of *AG*, were also undetected (data not shown).

Identification of potential stage markers

To initiate a global analysis, genes of known importance in anther development, such as the MADS-box factors discussed above, were picked as clustering seeds, and other transcripts with similar expression profiles in all three fertile lines were identified by hierarchical clustering. One pattern of interest are genes turned either completely on or off between the spikelet and anther stages. The first profile (Figure 5, cluster A) includes transcripts that were either turned down or off after stage S in fertile tissues. Most of these 45 genes are also downregulated in the mutants, although the mutants were not considered when generating this set; this reaffirms the relatively minor impact of these mutations at the S stage. At least 13 genes in this profile are putative transcription factors, including several MADS-box genes and *YABBY1/FILAMENTOUS FLOWER* (*FIL*) (Figure 6a; Data S6), which have been shown to function in floral meristem determination (Siegfried *et al.*, 1999). This set gradually decreases, as evident in the 'average expression level' bar graph (Figure 5a), possibly reflecting either a slow decay of pre-existing transcripts or a lowered transcription rate.

The second profile identified genes that were upregulated in A1.0 and contains three distinct clusters (Figure 5b–c). The 57 genes of cluster B includes examples that were expressed relatively normally in *mac1* and *ms23*, but not in *msca1* (Figure 5b). Within this cluster are genes required for the initiation of meiosis including *Dmc1* type B (TIGR:TC313913; Figure 6b), a maize *RAD51* homolog (Hamant *et al.*, 2006), and an *Argonaute/PIWI* homolog (TIGR:TC304331; Figure 6c). The T cytoplasm *male sterility restorter factor 2* gene (*Rf2*) is also in this group.

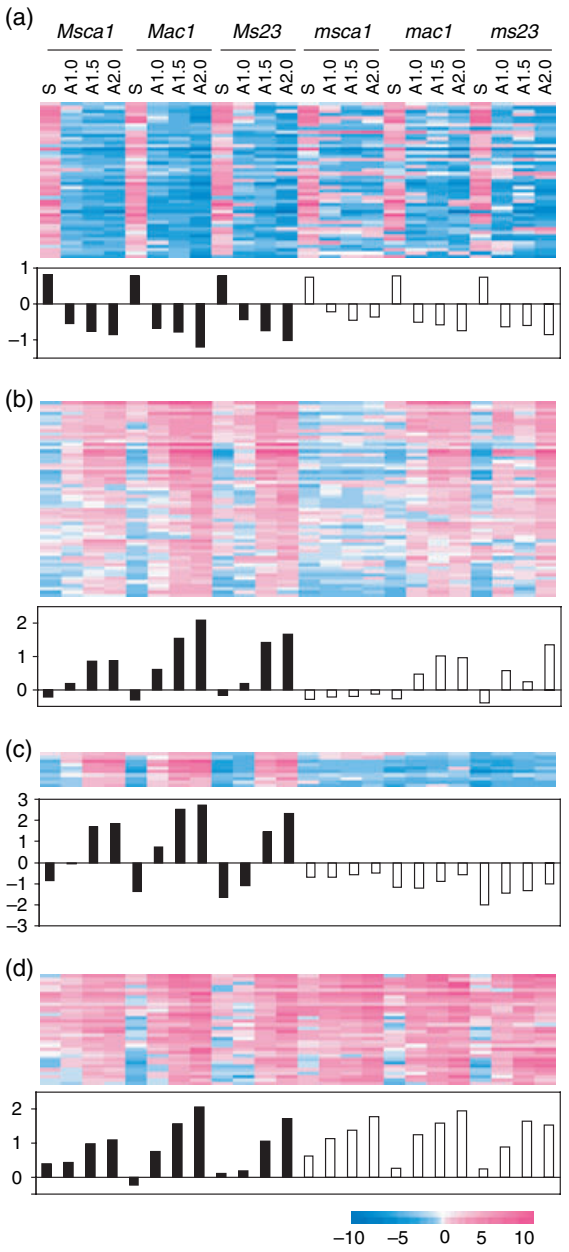

Figure 5. Clusters of potential stage markers. The fertile lines are *Msca1*, *Mac1* and *Ms23*. The color scale at the bottom of the figure displays the log-2 values of absolute intensities normalized over the median. Average expression values for the specified clusters (each column) are displayed as bar graphs.
(a) Transcripts either weakly expressed or turned off after the S stage. Panels (b) and (c) represent a class of transcripts that are induced after the S stage in all three fertile lines but are expressed differently in the mutants: (b) relatively normal in *mac1* and *ms23* but not *msca1*; (c) either missing or downregulated in all three mutants; (d) normal in all mutants. S, spikelets (including young anthers < 0.5 mm in length); A1.0, 1.0-mm anther; A1.5, 1.5-mm anther; A2.0, 2.0-mm anther.

Cluster C has 10 genes that were either missing or downregulated in all three *ms* mutants compared with fertile siblings (Figure 5c). As the primary characteristic shared among mutants is the lack of a tapetal layer

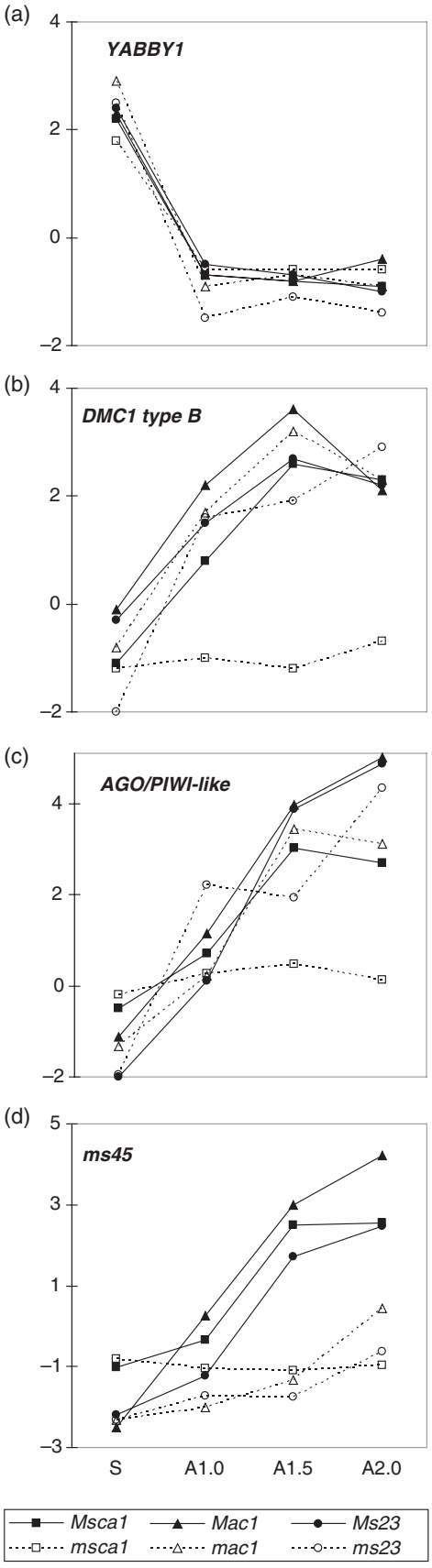

Figure 6. Expression profiles of four transcripts representative of clusters A–C in Figure 5. The expression values are averaged log-2 values of the absolute intensities normalized over the median value. The box at the bottom gives the six genotypes considered.
(a) *YABBY1* from cluster A (Figure 5a); (b) *DMC1* type B from cluster B (Figure 5b); (c) *AGO/PIWI*-like gene from cluster B; (d) *ms45*, from cluster C (Figure 5c).

(Figure 1b), this subgroup may be important for tapetal specification. This hypothesis is supported by inclusion of *ms45* (Figure 6d), a tapetal marker gene that is highly expressed during the early vacuolate microspore stage (Cigan *et al.*, 2001), and a putative β-1,3-glucanase (TIGR:TC289834), which is to be secreted by the tapetum during tetrad dissolution in microsporogenesis (Bucciaglia and Smith, 1994).

The 32 genes in cluster D are highly expressed after S and are not changed in the mutants (Figure 5d). This subgroup is highlighted by the *AG*-like gene *ZMM2* (TIGR:TC299558) and an *ECERIFERUM* (*CER1*) homolog (TIGR:TC307080). *ZMM2* is a C/D-type MADS-box gene required for maize floral determinacy (Mena *et al.*, 1996). *ZMM2* is clearly upregulated as the anther develops, and this trend remains the same in the mutants. In Arabidopsis, the *CER1* genes may function in wax biosynthesis, and the *cer1* mutant is conditionally male sterile (Aarts *et al.*, 1995).

At the A1.0 stage *mac1* anthers contain approximately 10-fold more archesporial derivatives than fertile anthers, but fewer than the normal number of parietal cell derivatives (Figure 1a; Sheridan *et al.*, 1999). Therefore, the *mac1* transcriptome might contain a class of transcripts that are significantly over-represented compared with fertile siblings and *ms23*, both of which contain wild-type numbers of archesporial derivatives. Furthermore, a subset of these transcripts would be expected to be either downregulated or missing in *msca1* anthers, where the archesporial derivatives differentiate into either parenchyma or vasculature. Surprisingly, we identified no transcripts fitting these criteria. It is possible that genes specific to archesporial proliferative cells were not represented on our arrays. The set of genes included in our arrays comprises ~25% of the total predicted number of maize genes, and includes 233 probes designed for maize cDNAs and EST sequences showing similarity to meiosis-associated genes from yeast and mouse. An alternative is that archesporial derivatives are defined primarily by their position in the anther, rather than by diagnostic gene expression patterns at the A1.0 stage, as predicted by a cell lineage model of specification of meiotic cells.

Expression profiles of two maize leucine-rich repeat receptor-like kinase homologs

In both Arabidopsis and rice, *mac1*-like mutants have been found. Mutations in *EXCESS MALE SPOROCYTES1/*

EXTRA SPOROGENOUS CELLS (*EMS1/EXS*) cause an excess of microsporocytes, which are proposed to originate from tapetum precursors (Zhao *et al.*, 2002). Mutations in the rice *MULTIPLE SPOROCYTE1* (*MSP1*) gene display very similar phenotypes (Nonomura *et al.*, 2003). *MSP1* and *EMS1/EXS* encode putative leucine-rich repeat receptor-like kinases (LRR-RLK), indicating the critical role of cell–cell signaling in sporogenesis. The rice and Arabidopsis mutants are similar to, but not precisely identical to, maize *mac1*, a gene that has not yet been cloned. To test the hypothesis that *mac1* is related to *MSP1*, the *ZmMSP1* homolog (Data S7a) was examined. The gene was expressed at a relatively high level in all three mutants (Data S7b), but in newly obtained *Mu*-tagged alleles of *mac1*, a PCR test for transposon insertion into *ZmMSP1* was negative (data not shown).

Given the importance of the LRR-RLKs in plant cell signaling, a maize homolog of the brassinolide receptor kinase, *brassinosteroid-insensitive1* (*BRI1*), termed *ZmBRI1* (Data S7a), was also identified. Brassinosteroids (BRs) are important in a wide range of plant developmental processes (reviewed in Wang and He, 2004). *BRI1* is expressed in many organs including developing flowers (Wang *et al.*, 2001). *ZmBRI1* displayed moderate and slowly decreasing expressions across the four stages, both in mutant and fertile anthers (Data S7c), indicating a potential early role of the plant steroid BR in maize anther development.

Conservation in expression of anther-specific genes

Endo *et al.* (2004) identified ~140 rice anther-specific genes using floral cDNA microarrays. By *in situ* hybridization, about 20 were tapetum-specific. In a correlation analysis (Data S8) the 20 putative maize orthologs are expressed at very comparable levels (Data S9a), indicating a remarkable conservation of gene regulation in cereal anther development. Quantitative expression levels were unchanged in the mutants (Data S9b). Considering that maize and rice diverged about 50 mya, this observation posits a very stringent selection on the regulation of floral organ differentiation.

Discussion

The maize tassel contains approximately 5000 anthers developing in synchronized cohorts over about 7 days. The absence of maturing female floral parts makes recovery of pure and carefully staged anthers relatively straightforward. These biological advantages were exploited to define the transcriptomes of normal fertile anthers, dissected only from the more advanced upper flower in each paired set covering the period of rapid mitotic proliferation, organization of internal cell layers and differentiation of cell types, including the sporocytes. To gain further insight into the progression of transcript types that underlie morphological change, three cell differentiation mutants were analyzed. *msca1* causes incorrect differentiation of all anther cell types, *mac1* causes an excess of sporocytes to develop at the expense of a normal tapetum and middle layer, and *ms23* lacks a differentiated tapetum. Both *mac1* and *ms23* mutants arrest at the beginning of meiosis. A large number of transcription factors and likely regulatory genes were identified that are predicted to play crucial roles in anther differentiation; a subset have reported mutant phenotypes very early in floral specification, illustrating the power of transcriptome profiling to identify genes with multiple periods of expression obscured by early developmental arrest in mutants.

A key finding from this study is that stamen and organ identity MADS-box genes of the ABC model are expressed normally at all four stages in the mutants. It has been known that some of the MADS-box genes are expressed throughout development in the organs they specify (Jack, 2004). It was unexpected that so many of these genes were expressed, some at persistently high levels, throughout the early development of fertile and sterile anthers. All cell layers in the *msca1* anther are transformed (Chaubal *et al.*, 2003), yet these stamen specification genes are still sustained at the wild-type levels, with the exceptions of the C function genes *ZAG1* and *ZMM2*. Expression of *AG* is under the control of multiple positive and negative regulatory mechanisms (Ma, 2005). Therefore, the upregulation of *ZAG1* and *ZMM2* in *msca1* anthers may result from the loss of a repressing mechanism, in addition to the hypothesized repression of leaf developmental genes.

The interplay between lineage and cell–cell interaction in floral organogenesis

A strict lineage determination explanation for cell fate acquisition is unlikely. Cell–cell interaction and signaling are favored because some floral organ identity genes function non-cell-autonomously (Jenik and Irish, 2001; Sessions *et al.*, 2000). Despite this, sporogenous cell differentiation has been proposed to depend on features intrinsic to archesporial cells and meiocytes (Goldberg *et al.*, 1993), although the role of the surrounding cells has not yet been fully studied. In fact, in the ovule, the megasporocyte carries out meiosis without the support of any specific cell layers like those found in the anther. One important piece of evidence for the hypothesis of meiotic cell autonomy comes from the *ameiotic1* (*am1*) mutant of maize (Golubovskaya *et al.*, 1993), in which all cell layers differentiate normally but sporogenous cells conduct mitosis instead of meiosis. Therefore signals from normal somatic cells appear to be insufficient to ensure meiosis. The fact that two of the three mutants analyzed in this study, *mac1* and *ms23*, can also initiate meiosis normally without a functional tapetum provides further evidence for this conclusion. In contrast, the

failure to complete meiosis in these two mutants suggests that neighboring cells play a crucial role during meiosis, either in signaling or in nutrition, another form of cell–cell interaction.

At the beginning of L2 proliferation, hypodermal cell division establishes archesporial and parietal cells by unknown mechanisms (Ma, 2005). Asymmetric placement or distribution of hypodermal cell structures could establish these two cell types; if true, then a lineage decision early in ontogeny must be reinforced and clarified later to sustain normal development.

One insight into the cell-fate determining processes was provided by the discovery that *AG* controls microsporogenesis through the activation of the *SPOROCYTELESS/NOZZLE* (*SPL/NZZ*) gene in the very early stages of Arabidopsis anther development (Ito *et al.*, 2004), but is not required for *SPL/NZZ* function in sporogenesis induction once it is activated. Interestingly, both maize and rice lack a homolog to the SPL/NZZ nuclear protein. This suggests regulation of microsporogenesis in maize, and perhaps grasses or even monocots in general, is not directly analogous to Arabidopsis. Phenotypically, the *spl/nzz* mutant in Arabidopsis produces anthers containing vacuolated parenchymal cells and no microsporocytes, superficially similar to the *msca1* phenotype. However, *spl/nzz* is both male- and female-sterile (Balasubramanian and Schneitz, 2000), whereas *msca1* is female-fertile (Chaubal *et al.*, 2003). Therefore the *msca1* gene may function differently than *SPL/NZZ*, or alternatively, a new gene has evolved to induce sporogenesis in the maize ovule, analogous to the case of the duplicated *AG* homologs, *ZAG1* and *ZMM2*.

The archesporial cells may also regulate the cellular fate of the other cell types through cell–cell signaling. The three *ms* mutants provide some evidence for this hypothesis. The stamen primordia are initiated normally in all three mutants (Chaubal *et al.*, 2000, 2003; Sheridan *et al.*, 1999). In *msca1* the filament is normal, but all cells in the *msca1* 'anther' are transformed including the epidermis, which looks normal in the early stages but develops stomata later (Chaubal *et al.*, 2003). A logical hypothesis is that *msca1* encodes a repressor of leaf development that acts at the A1.0 stage or earlier; in normal anthers some leaf development genes are transiently expressed at this stage (Ma *et al.*, 2006). The late differentiation of guard cells in the epidermis suggests that, as in leaves, the L2 hypodermal cells are important in this differentiation. *msca1*, or more likely, one of its downstream targets, may be expressed in the L2 and act on the epidermis. One example of this mechanism is the *AP3* MADS-box gene. In Arabidopsis, the normal epidermal-cell-type differentiation requires the expression of *AP3* in the underlying L2 cell layer (Jenik and Irish, 2001). The high expression of *Si1*, the maize ortholog of *AP3*, at a normal level did not prevent the *msca1* anther epidermis from transforming, implying that the *msca1* gene might be working downstream of *Si1*.

The *mac1* gene may also work in a similar non-cell-autonomous manner, if its expression is restricted to the archesporial cells (Sheridan *et al.*, 1999). It has been suggested that archesporial cells promote periclinal division in the primary parietal layer and the inner secondary parietal layer, as only the cell layer adjacent to the archesporium undergoes periclinal divisions. This interpretation of *mac1* can explain both the lack of periclinal divisions in the primary parietal cells, and the apparent excessive division of the archesporial cells (Sheridan *et al.*, 1999). Similarly, the lack of the *ms23* gene function could result in the abnormal extra division in the tapetal cell precursors, and hence tapetal failure.

Taken together, a simple model emerges in which a few genes, such as the MADS-box set, establish differences between archesporial and other L2 cells at the very early stages of anther organogenesis, maybe at the first division of the hypodermal cell. These cells could then produce a gradient of morphogens progressively refining cell type specifications within the L2 derivatives to ensure the archesporial cells differentiate into microsporocytes. Evidence from genetic analysis of other *ms* mutants points to an even more flexible 'late' determinative model for microsporogenesis. The excess microsporocytes from *ems/exs* mutants are proposed to have originated from the tapetum precursors (Zhao *et al.*, 2002), suggesting the capacity to assume a meiotic fate is retained multiple generations after the initial periclinal division by the hypodermal cell layer.

Another piece of evidence for a late determinative model is provided by the expression profiles of a set of meiosis-associated genes. Of the 233 probes included, 142 displayed detectable hybridizations. Surprisingly, most of these genes were expressed at normal levels in all three mutants (Data S10a–c), with the exception of *msca1* tissues, where the general trend was towards downregulation at all four stages (Data S10d). Therefore, the transcriptional competence to undergo meiosis may be present in all L2 cells in the maize anther.

In conclusion, transcriptome profiling of maize mutants with alterations in cell type specification and differentiation in the anther is shown to be valuable in identifying genes differentially expressed at specific stages of anther development. Given the cell specification defects in each mutant, subsets of genes differentially expressed in mutants are either cell-type specific marker genes or markers for the responses of cells to differentiation by neighboring cells. As there are more than 350 male-sterile mutants in maize not yet classified cytologically, it is highly likely that additional mutations affecting cell type specification prior to meiosis can be identified to extend this analysis. Additionally, both forward and reverse genetic strategies can be used to initiate

the study of specific functions of the genes identified in this study.

Experimental procedures

Biological materials

The *msca1* and *ms23* lines were from P. Bedinger (Colorado State, Ft. Collins, CO) and *mac1* was from W. Sheridan (The University of North Dakota, Fargo, ND). Families were grown at Stanford University in summer 2003; *ms23* and *msca1* were crossed by W23, followed by a self-pollination, and *mac1* was crossed by fertile siblings. Samples were collected from the summer 2004 field by cutting into the plant and removing tassel branches (Ma *et al.*, 2006). Because there are differences in the rate of development of upper and lower florets, only the upper florets were used for anther dissection. At maturity, pollen shed was scored to determine the fertility of individuals.

Array design and data analysis

The Version 2 maize oligonucleotide array was designed at Stanford and produced by Agilent (http://www.home.agilent.com). The array contains 22 575 probes, including 1450 internal positive controls, 162 internal negative controls and 20 963 gene features. More than 80% of the gene probes were from Version 1 arrays; new probes were designed from ~3000 maize complete cDNA or EST sequences from GenBank. To identify unique genes or transcripts, the probe set was mapped to the latest TIGR Maize Gene Index (Release 16.0, October 2005; http://www.tigr.org/tigr-scripts/tgi/T_index.cgi?species=maize; as of January 2007, the Gene Index databases are being moved to the Dana-Farber Cancer Institute; http://compbio.dfci.harvard.edu/tgi/). In total, ~13 000 unique sense and ~5000 unique antisense transcripts are represented (see Ma *et al.*, 2006 for methods used to determine antisense transcripts). Array hybridization and data analysis were carried out as described in Ma *et al.* (2006), except for these modifications. After determining the thresholds for background hybridizations for each array, and choosing probes with above-threshold intensities in at least two out of the three independent biological duplicates as the 'above-background' subset, these 'above-background' subsets were combined for each hybridization type (12 fertile:*ms* pairs), generating a 'hybridized' collection of ~12 000–14 000 probes. Only these 'hybridized' probes were subjected to the normalization procedure as described in Ma *et al.* (2006). After normalization and outlier removal by a Grubb's test ($p = 0.01$), a probe is called 'present' if it was 'hybridized' in all three fertile lines (siblings of the three *ms* mutants) at any given anther stage. This was carried out to remove potential line-specific variations that may interfere with downstream data analysis. The 'all-present' set includes 10 693 probes representing ~9200 unique transcripts (both sense and antisense). Normalized expression values for a given probe were calculated as *log-2(normalized intensity/median of the 10 693 probes on the array)* and then averaged across the three biological replicates. Probe sequences, gene identities and both raw and normalized hybridization intensities for each probe can be downloaded from the Gene Expression Omnibus database (http://www.ncbi.nlm.nih.gov/geo/). To assess differential expression, the Rank Products method (Breitling *et al.*, 2004) was used as described previously (Ma *et al.*, 2006). Hierarchical clustering of expressed transcripts was performed with EPCLUST (http://ep.ebi.ac.uk/EP/EPCLUST), using correlation measure based distance and average linkage clustering methods. All statistical analyses were performed using either the R package (http://www.r-project.org/) or Microsoft EXCEL (http://www.microsoft.com).

Quantitative real-time PCR

Real-time PCR experiments were carried out as described in Ma *et al.* (2006). Briefly, PCR primers were designed using Primer 3 (http://frodo.wi.mit.edu/cgi-bin/primer3/primer3_www.cgi) using default parameters and synthesized by Illumina (http://www.illumina.com). Primer sets were as follows: histone acetyltransferase (GCN5; TIGR:TC326475), forward primer, 5′-GCCGACATGAAGAGAATGTT-3′, reverse, 5′-CAGCCTAGCTCTTGGTTGAG-3′; helicase-domain containing gene (GenBank:BG833488), forward, 5′-GTATGATGGAAGGCGAGAAG-3′, reverse, 5′-CACTCCTGTCTGATGTTGGA-3′; cyanate hydratase (cyanase; TIGR:TC330555), forward, 5′-GCTGGTGAGGAGGAGAAACA-3′, reverse, 5′-CAGCAATCATGCCAGGTAGA-3′; and *UBC* (GenBank: BG836869), forward, 5′-CGACAGGGCCAAGTATGAGT-3′, reverse, 5′-TGCACAATGGTCCTCAAAAG-3′. Extra biological samples were used in addition to the same samples used for array hybridizations. PCR product specificity and size were verified by melting curve analysis for all reactions and gel electrophoresis for a subset of reactions. All four products were also sequenced to ensure the correct transcripts were amplified (data not shown). Primer efficiency was validated by using the 'DART-PCR midpoint' method (Peirson *et al.*, 2003), and ANOVA outliers for efficiency and expression were removed in DART-PCR before the C_t values were used for the correlation analysis.

Acknowledgements

We thank Lisa Harper and Rachel Wang for contributing the meiosis-related maize gene list, Inna Golubovskaya for sharing cytological insights about *mac1*, and Sam Stingley and Gene Tanimoto for training and assistance with the Affymetrix platform. Supported by the National Science Foundation (98-72657). JM was supported partially by a National Library of Medicine Genome Training Grant awarded to the Stanford Biomedical Informatics Program.

Supplementary Material

The following supplementary material is available for this article online:

Data S1. Correlations between the Agilent array results and the Affymetrix platform results.

Data S2. Differentially expressed transcripts in the three *ms* mutants at the four stages.

Data S3. Average linkage clustering trees for both fertile and *ms* mutant tissues.

Data S4. Test for misexpression of leaf genes in mutant anthers.

Data S5. Differentially expressed transcripts in the three *ms* mutants that are also highly expressed in leaf.

Data S6. Lists of genes in the four clusters analyzed in Figure 5.

Data S7. Putative maize leucine-rich repeat receptor-like kinase (LRR-RLK) genes.

Data S8. Maize orthologs of rice anther-expressed genes.

Data S9. Conservation of gene expression regulation between maize and rice anther-specific orthologs.

Data S10. Relative expression levels (Ex) of 142 meiosis-related transcripts on the array.

References

Aarts, M.G., Keijzer, C.J., Stiekema, W.J. and Pereira, A. (1995) Molecular characterization of the *CER1* gene of *Arabidopsis* involved in epicuticular wax biosynthesis and pollen fertility. *Plant Cell*, **7**, 2115–2127.

Ambrose, B.A., Lerner, D.R., Ciceri, P., Padilla, C.M., Yanofsky, M.F. and Schmidt, R.J. (2000) Molecular and genetic analyses of the *silky1* gene reveal conservation in floral organ specification between eudicots and monocots. *Mol. Cell*, **5**, 569–579.

Balasubramanian, S. and Schneitz, K. (2000) NOZZLE regulates proximal-distal pattern formation, cell proliferation and early sporogenesis during ovule development in *Arabidopsis thaliana*. *Development*, **127**, 4227–4238.

Barnes, M., Freudenberg, J., Thompson, S., Aronow, B. and Pavlidis, P. (2005) Experimental comparison and cross-validation of the Affymetrix and Illumina gene expression analysis platforms. *Nucleic Acids Res.* **33**, 5914–5923.

Breitling, R., Armengaud, P., Amtmann, A. and Herzyk, P. (2004) Rank products: a simple, yet powerful, new method to detect differentially regulated genes in replicated microarray experiments. *FEBS Lett.* **573**, 83–92.

Bucciaglia, P.A. and Smith, A.G. (1994) Cloning and characterization of *Tag 1*, a tobacco anther beta-1,3-glucanase expressed during tetrad dissolution. *Plant Mol. Biol.* **24**, 903–914.

Chaubal, R., Zanella, C., Trimnell, M.R., Fox, T.W., Albertsen, M.C. and Bedinger, P. (2000) Two male-sterile mutants of *Zea Mays* (Poaceae) with an extra cell division in the anther wall. *Am. J. Bot.* **87**, 1193–1201.

Chaubal, R., Anderson, J.R., Trimnell, M.R., Fox, T.W., Albertsen, M.C. and Bedinger, P. (2003) The transformation of anthers in the *msca1* mutant of maize. *Planta*, **216**, 778–788.

Cigan, A.M., Unger, E., Xu, R.-., Kendall, T. and Fox, T.W. (2001) Phenotypic complementation of *ms45* maize requires tapetal expression of *MS45*. *Sex Plant Reprod.* **14**, 135–142.

Czechowski, T., Stitt, M., Altmann, T., Udvardi, M.K. and Scheible, W.R. (2005) Genome-wide identification and testing of superior reference genes for transcript normalization in *Arabidopsis*. *Plant Physiol.* **139**, 5–17.

Endo, M., Tsuchiya, T., Saito, H. *et al.* (2004) Identification and molecular characterization of novel anther-specific genes in *Oryza sativa* L. by using cDNA microarray. *Genes Genet. Syst.* **79**, 213–226.

Goldberg, R.B., Beals, T.P. and Sanders, P.M. (1993) Anther development: basic principles and practical applications. *Plant Cell*, **5**, 1217–1229.

Golubovskaya, I., Grebennikova, Z.K., Avalkina, N.A. and Sheridan, W.F. (1993) The role of the *ameiotic1* gene in the initiation of meiosis and in subsequent meiotic events in maize. *Genetics*, **135**, 1151–1166.

Hamant, O., Ma, H. and Cande, W.Z. (2006) Genetics of meiotic prophase I in plants. *Annu. Rev. Plant Biol.* **57**, 267–302.

Irish, V.F. and Jenik, P.D. (2001) Cell lineage, cell signaling and the control of plant morphogenesis. *Curr. Opin. Genet. Dev.* **11**, 424–430.

Ito, T., Wellmer, F., Yu, H., Das, P., Ito, N., Alves-Ferreira, M., Riechmann, J.L. and Meyerowitz, E.M. (2004) The homeotic protein AGAMOUS controls microsporogenesis by regulation of *SPOROCYTELESS*. *Nature*, **430**, 356–360.

Jack, T. (2004) Molecular and genetic mechanisms of floral control. *Plant Cell*, **16**(Suppl.), S1–S17.

Jenik, P.D. and Irish, V.F. (2001) The *Arabidopsis* floral homeotic gene *APETALA3* differentially regulates intercellular signaling required for petal and stamen development. *Development*, **128**, 13–23.

Ma, H. (2005) Molecular genetic analyses of microsporogenesis and microgametogenesis in flowering plants. *Annu. Rev. Plant Biol.* **56**, 393–434.

Ma, J., Morrow, D.J., Fernandes, J. and Walbot, V. (2006) Comparative profiling of the sense and antisense transcriptome of maize lines. *Genome Biol.* **7**, R22.

Mena, M., Ambrose, B.A., Meeley, R.B., Briggs, S.P., Yanofsky, M.F. and Schmidt, R.J. (1996) Diversification of C-function activity in maize flower development. *Science*, **274**, 1537–1540.

Munster, T., Wingen, L.U., Faigl, W., Werth, S., Saedler, H. and Theissen, G. (2001) Characterization of three *GLOBOSA*-like MADS-box genes from maize: evidence for ancient paralogy in one class of floral homeotic B-function genes of grasses. *Gene*, **262**, 1–13.

Nonomura, K., Miyoshi, K., Eiguchi, M., Suzuki, T., Miyao, A., Hirochika, H. and Kurata, N. (2003) The *MSP1* gene is necessary to restrict the number of cells entering into male and female sporogenesis and to initiate anther wall formation in rice. *Plant Cell*, **15**, 1728–1739.

Peirson, S.N., Butler, J.N. and Foster, R.G. (2003) Experimental validation of novel and conventional approaches to quantitative real-time PCR data analysis. *Nucleic Acids Res.* **31**, e73.

Schmidt, R.J., Veit, B., Mandel, M.A., Mena, M., Hake, S. and Yanofsky, M.F. (1993) Identification and molecular characterization of *ZAG1*, the maize homolog of the *Arabidopsis* floral homeotic gene *AGAMOUS*. *Plant Cell*, **5**, 729–737.

Sessions, A., Yanofsky, M.F. and Weigel, D. (2000) Cell-cell signaling and movement by the floral transcription factors *LEAFY* and *APETALA1*. *Science*, **289**, 779–782.

Sheridan, W.F., Golubeva, E.A., Abrhamova, L.I. and Golubovskaya, I.N. (1999) The *mac1* mutation alters the developmental fate of the hypodermal cells and their cellular progeny in the maize anther. *Genetics*, **153**, 933–941.

Siegfried, K.R., Eshed, Y., Baum, S.F., Otsuga, D., Drews, G.N. and Bowman, J.L. (1999) Members of the *YABBY* gene family specify abaxial cell fate in *Arabidopsis*. *Development*, **126**, 4117–4128.

Walbot, V. and Petrov, D.A. (2001) Gene galaxies in the maize genome. *Proc. Natl Acad. Sci. USA*, **98**, 8163–8164.

Wang, Z.Y. and He, J.X. (2004) Brassinosteroid signal transduction – choices of signals and receptors. *Trends Plant Sci.* **9**, 91–96.

Wang, Z.Y., Seto, H., Fujioka, S., Yoshida, S. and Chory, J. (2001) BRI1 is a critical component of a plasma-membrane receptor for plant steroids. *Nature*, **410**, 380–383.

Whipple, C.J., Ciceri, P., Padilla, C.M., Ambrose, B.A., Bandong, S.L. and Schmidt, R.J. (2004) Conservation of B-class floral homeotic gene function between maize and *Arabidopsis*. *Development*, **131**, 6083–6091.

Zhao, D.Z., Wang, G.F., Speal, B. and Ma, H. (2002) The *excess microsporocytes1* gene encodes a putative leucine-rich repeat receptor protein kinase that controls somatic and reproductive cell fates in the *Arabidopsis* anther. *Genes Dev.* **16**, 2021–2031.

